

1 CAMELS-DE: hydro-meteorological time series and attributes for 2 1582 catchments in Germany

3 Ralf Loritz*¹, Alexander Dolich*¹, Eduardo Acuña Espinoza^{1,A}, Pia Ebeling^{2,A}, Björn Guse^{3,4,A}, Jonas
4 Götte^{5,6,7,A}, Sibylle K. Hassler⁸, Corina Hauffe^{9,A}, Ingo Heidebüchel^{2,10,A}, Jens Kiesel^{3,11,A}, Mirko
5 Mälicke^{1,A}, Hannes Müller-Thomy^{12,A}, Michael Stölzle^{13,A}, Larisa Tarasova^{14,A}

6

7 *equal contribution, A alphabetic order

8 ¹Karlsruhe Institute of Technology (KIT), Institute for Water and Environment, Karlsruhe, Germany

9 ²Helmholtz Centre for Environmental Research - UFZ, Department Hydrogeology, Leipzig, Germany

10 ³Kiel University, Hydrology and Water Resources Management, Kiel, Germany

11 ⁴German Research Centre for Geosciences - GFZ Potsdam, Section Hydrology, Potsdam, Germany

12 ⁵WSL Institute for Snow and Avalanche Research SLF, Davos Dorf, Switzerland

13 ⁶Climate Change, Extremes and Natural Hazards in Alpine Regions Research Center CERC, Davos Dorf

14 ⁷Institute for Atmospheric and Climate Science, ETH Zurich, Zurich, Switzerland

15 ⁸Karlsruhe Institute of Technology (KIT), Institute of Meteorology and Climate Research - Atmospheric Trace Gases and
16 Remote Sensing (IMK-ASF), Karlsruhe, Germany

17 ⁹University of Technology Dresden (TUD), Institute of Hydrology and Meteorology, Dresden, Germany

18 ¹⁰Bayreuth Centre of Ecology and Environmental Research, University of Bayreuth, Bayreuth, Germany

19 ¹¹Stone Environmental, 535 Stone Cutters Way, 05602 Montpelier (VT), USA

20 ¹²Technische Universität Braunschweig, Leichtweiß-Institute for Hydraulic Engineering and Water Resources, Division of
21 Hydrology and River Basin Management, Braunschweig, Germany

22 ¹³Chair of Hydrology, University of Freiburg, Freiburg, Germany, now at: LUBW Landesanstalt für Umwelt (State Agency
23 for Environment), Karlsruhe, Germany

24 ¹⁴Helmholtz Centre for Environmental Research - UFZ, Department Catchment Hydrology, Germany

25

26 *Correspondence to:* Ralf Loritz (Ralf.Loritz@kit.edu) and Alexander Dolich (Alexander.Dolich@kit.edu)

27 **Abstract.** Comprehensive large sample hydrological datasets, particularly the CAMELS datasets (Catchment Attributes and
28 Meteorology for Large-sample Studies), have advanced hydrological research and education in recent years. These datasets
29 integrate extensive hydro-meteorological observations with landscape features, such as geology and land use, across
30 numerous catchments within a national framework. They provide harmonised large sample data for various purposes, such as
31 assessing the impacts of climate change or testing hydrological models on a large number of catchments. Furthermore, these

32 datasets are essential for the rapid progress of data-driven models in hydrology in recent years. Despite Germany's extensive
33 hydro-meteorological measurement infrastructure, it has lacked a consistent, nationwide hydrological dataset, largely due to
34 its decentralised management across different federal states. This fragmentation has hindered cross-state studies and made
35 the preparation of hydrological data labour-intensive. The introduction of CAMELS-DE represents a step forward in
36 bridging this gap. CAMELS-DE includes 1582 streamflow gauges with hydro-meteorological time series data covering up to
37 70 years (median length of 46 years and a minimum length of 10 years), from January 1951 to December 2020. It includes
38 consistent catchment boundaries with areas ranging from 5 to 15,000 km² along with detailed catchment attributes covering
39 soil, land cover, hydrogeologic properties and data about human influences. Furthermore, it includes a regionally trained
40 Long-Short Term Memory (LSTM) network and a locally trained HBV (Hydrologiska Byråns Vattenbalansavdelning) model
41 that were used as quality control and that can be used to fill gaps in discharge data or act as baseline models for the
42 development and testing of new hydrological models. Given the large number of catchments, including numerous relatively
43 small ones (636 catchments < 100 km²), and the time series length of up to 70 years (166 catchments with 70 years of
44 discharge data), CAMELS-DE is one of the most comprehensive national CAMELS datasets available and offers new
45 opportunities for research, particularly in studying long-term trends, runoff formation in small catchments and in analysing
46 catchments with strong human influences.

47 **1 Introduction**

48 The CAMELS (Catchment Attributes and MEteorology for Large-sample Studies) datasets have become a cornerstone
49 within the hydrological community for their comprehensive and consistent integration of hydro- and meteorological data
50 across entire countries, including the USA, UK, Australia, Brazil, Chile, and others (e.g. Addor et al., 2017, Coxon et al.,
51 2020). These datasets combine catchment attributes (e.g. land use, geology, and soil properties), hydrological time series
52 (e.g. water level and discharge), and meteorological time series (e.g. precipitation and temperature) for a multitude of
53 catchments typically within a single country. A distinctive feature of CAMELS datasets is their role as a benchmark for
54 hydrological modelling and large sample analysis, enabling the comparison of hydrological models and the validation of
55 water resources management strategies across diverse landscapes and climates (Brunner et al., 2021). Particularly the
56 CAMELS-US dataset has thereby formed the basis for the on-going rise of machine learning methods in hydrology (e.g
57 Kratzert et al., 2019).

58

59 Despite the widespread adoption and utility of CAMELS datasets in research, teaching, and practical applications globally,
60 Germany with its extensive hydro-meteorological measurement network has no comprehensive and harmonised dataset yet.
61 While there are large sample hydrological datasets that cover either parts of Germany (Klingler et al., 2021), only a fraction
62 of the available national hydrological data (Färber et al., 2023), or focus on catchment water quality and thus cover a lower
63 sampling frequency (Ebeling et al., 2022), the absence of a full CAMELS dataset that includes harmonised, daily,

64 high-quality national hydrological and meteorological data together with catchment attributes and catchment boundaries
65 derived from national and international products limits the potential for comprehensive analyses and advancements in
66 hydrological research and practice. The CAMELS-DE data set addresses this gap (Dolich et al., 2024). CAMELS-DE
67 compiles discharge, water levels, catchment attributes, and catchment boundaries together with a suite of meteorological
68 time series and catchment attributes for 1582 catchments across Germany. Furthermore, the dataset includes discharge
69 simulations from two sources: a regionally-trained Long-Short Term Memory (LSTM) network (Hochreiter & Schmidhuber,
70 1997; Hochreiter, 1998), and a locally trained conceptual HBV model (Hydrologiska Byråns Vattenbalansavdelning,
71 Bergström and Forsman, 1973, Seibert, 2005, Feng et al., 2022). These simulations can serve as a benchmark for future
72 hydrological modelling studies in Germany or help fill data gaps in hydrological time series. Each component of the
73 CAMELS-DE processing pipeline is fully containerized (see section 7), which solves code dependency issues and generally
74 contributes to the traceability, comprehensiveness, and reproducibility of the generation of CAMELS-DE. This study
75 introduces not only a comprehensive dataset but also a suite of tools designed to generate reproducible hydrological datasets
76 from the provided raw data. In the following sections we provide a comprehensive description of all data contained within
77 CAMELS-DE including (1) its source data, (2) how the time series and attributes were produced, and (3) a discussion of the
78 associated limitations and uncertainties. The structure of this paper (and also the corresponding dataset) closely mirrors that
79 of the CAMELS-UK (Coxon et al., 2020) and CAMELS-CH (Höge et al., 2023) studies, ensuring comparability of the
80 datasets while maintaining distinct elements that are not identical but closely related.

81 **2 Data sources and providers**

82 CAMELS-DE brings together hydrological data, consisting of daily measurements of discharge ($\text{m}^3 \text{s}^{-1}$) and water levels (m),
83 from thirteen German federal state agencies, namely the Landesanstalt für Umwelt Baden-Württemberg (LUBW,
84 Nomenclature of Territorial Units for Statistics (NUTS) Level 1: DE1), Bayerisches Landesamt für Umwelt (LfU-Bayern,
85 DE2), Landesamt für Umwelt Brandenburg (LfU-Brandenburg, DE4), Hessisches Landesamt für Naturschutz, Umwelt und
86 Geologie (HLNUG, DE7), Landesamt für Umwelt, Naturschutz und Geologie Mecklenburg-Vorpommern (LUNG MV,
87 DE8), Niedersächsischer Landesbetrieb für Wasserwirtschaft, Küsten- und Naturschutz, Landesamt für Natur (NLWKN,
88 DE9), Umwelt und Verbraucherschutz Nordrhein-Westfalen (LANUV NRW, DEA), Landesamt für Umwelt Rheinland-Pfalz
89 (LUA-Rheinland Pfalz, DEB), Landesamt für Umwelt- und Arbeitsschutz Saarland (LUA, DEC), Landesamt für Umwelt,
90 Landwirtschaft und Geologie Sachsen (LfULG, DED), Landesamt für Umweltschutz Sachsen-Anhalt (LAU, DEE),
91 Landesamt für Landwirtschaft, Umwelt und ländliche Räume Schleswig-Holstein (LLUR, DEF), and Thüringer Landesamt
92 für Umwelt, Bergbau und Naturschutz (TLUBN, DEG). The only federal states not included are the city-states of Bremen,
93 Hamburg, and Berlin, which together account for less than 0.6 % of Germany's area, ensuring that the CAMELS-DE dataset
94 remains representative for Germany.

95

96 Meteorological data, specifically precipitation, temperature, relative humidity and radiation, were obtained from the German
97 Weather Service (DWD) from the HYRAS dataset (DWD-HYRAS, 2024). Spatially aggregated catchment attributes were
98 obtained from various sources. From the European Union, we incorporated open-access datasets from Copernicus, the EU's
99 Earth observation program, in particular the Copernicus GLO-30 DEM (Global 30-meter Digital Elevation Model;
100 EU-DEM, 2022) for information about topography and the CORINE Land Cover 2018 dataset (CLC, 2018) for information
101 about land cover. Soil attributes were derived from the global SoilGrids250m dataset (Poggio et al., 2021). Hydrogeological
102 catchment attributes were derived from the “Hydrogeologische Übersichtskarte von Deutschland 1:250.000” (HGM250,
103 2019) provided by the Bundesanstalt für Geowissenschaften und Rohstoffe (BGR) while information about human
104 influences, e.g. dams or weirs, was sourced from Speckhann et al. (2021).

105 **3 Catchments**

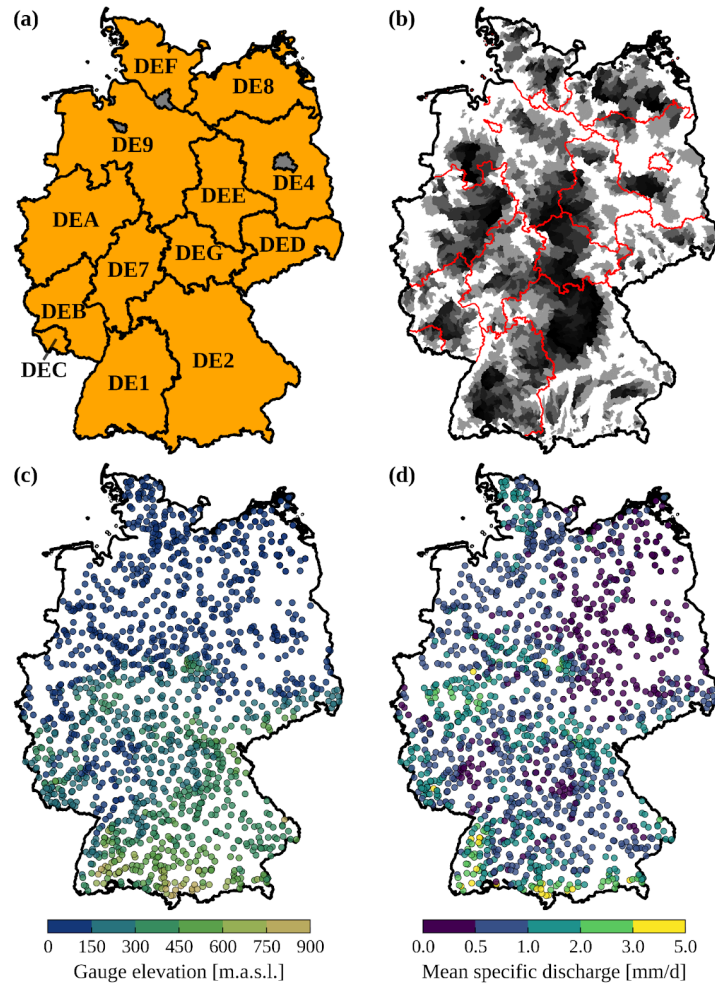
106 For CAMELS-DE, we sourced discharge ($\text{m}^3 \text{s}^{-1}$), water level data (m) and metadata for 2964 gauges and water level stations
107 from the different federal state agencies (see section 2). We created a subset of the data by selecting only measurement
108 stations that contained all required information, such as gauge name, location and catchment area in their metadata ($n = 2700$
109 stations), have at least a total of 10 years of discharge data, which must not necessarily be continuous ($n = 2227$ stations),
110 have a catchment area larger than 5 km^2 and smaller than $15,000 \text{ km}^2$ ($n = 2586$ stations), have a catchment area located
111 entirely within the borders of Germany ($n = 2298$ stations) and where the derived catchment area does not differ more than
112 20 % from the reported value by the federal states ($n = 2164$ stations; see section 3.1). These requirements were established
113 based on the following rationale: A minimum of 10 years of discharge data is necessary to ensure an adequate time series
114 length for hydrological modelling and calculating hydrological signatures. The minimum catchment area of 5 km^2 was
115 chosen to match the $1 \times 1 \text{ km}$ resolution of the precipitation raster product, ensuring that multiple raster cells intersect with
116 the catchment boundary. The upper limit was set because catchments larger than $15,000 \text{ km}^2$ are predominantly influenced
117 by human activities and often extend beyond Germany's borders, necessitating their exclusion. The 20 % discrepancy
118 between derived and reported catchment areas was arbitrarily chosen as an acceptable threshold for mass balance errors. This
119 threshold prevents the inclusion of catchments with significantly inaccurate delineations while avoiding the exclusion of too
120 much data (see Fig. 2b). Catchments partially located outside Germany's borders were excluded to avoid complications with
121 cross-border data, especially given the absence of open, high-quality meteorological data from the DWD beyond Germany's
122 national borders from 1951 to 2020. These criteria resulted in a subset of 1582 gauges for the CAMELS-DE dataset, which
123 provides a reliable representation of hydrological processes in Germany (Fig. 1c, d).

124 **3.1 Catchment boundaries**

125 Not all state authorities provided official catchment boundaries for their gauging stations, and the methods used by the
126 federal states to derive these boundaries are not uniform and remain unclear. Therefore, we tested two different global

127 catchment datasets, HydroSHEDS (Lehner et al., 2021) and MERIT Hydro (Yamazaki et al., 2019), to derive a consistent set
128 of catchment boundaries across Germany for the CAMELS-DE dataset. For that we compared the catchment areas
129 determined with HydroSHEDS and MERIT Hydro to the catchment areas reported by the state authorities. This comparison
130 was possible because all federal states shared the area of the catchments while not always sharing the actual catchment
131 boundaries. Overall, the comparison revealed that MERIT Hydro has lower errors between the reported and derived
132 catchment areas compared to HydroSHEDS. Among other reasons, this is because MERIT Hydro derives the catchment
133 boundaries directly at the gauge locations provided by the federal states (see section 3.2). The comparison between MERIT
134 Hydro and HydroSHEDS was further supported by extensive manual assessments, involving the visual inspection of
135 numerous catchments to evaluate their shapes and alignments in case the federal state provided the data. Consequently,
136 MERIT Hydro was used for the derivation of catchment boundaries for CAMELS-DE. Note that the derivation of the
137 catchment boundaries is a major source of uncertainty as the meteorological time series and the catchment attributes are
138 dependent on the catchment boundaries. To minimise the uncertainty of the catchment delineation we only included
139 catchments with a deviation of up to 20 percent from the catchment area reported by the federal agencies (Fig. 2b). We report
140 the original catchment area as (area_metadata) and the MERIT-Hydro based area (area) in the table of topographic attributes
141 (Table 2).

142



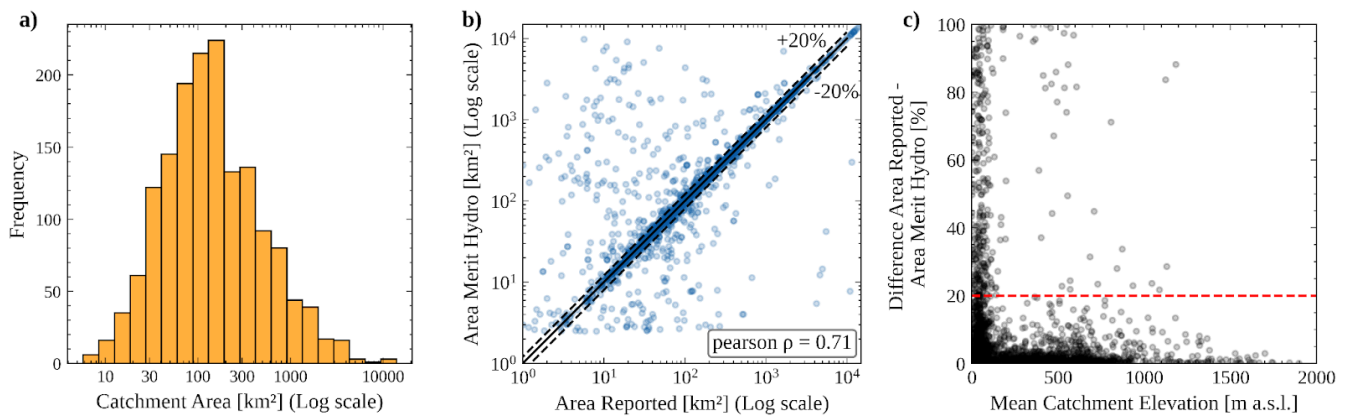
143

144 **Figure 1:** Panel (a) shows the German federal states labelled with their NUTS Level 1 ID as used for the CAMELS-DE gauge IDs. Panel (b) shows all 1582
 145 catchments provided in CAMELS-DE, the geometries of the catchments are shown transparently, so a darker colour means that the geometries of the
 146 catchments in that area overlap; the darker the colour, the higher the density of catchments in that area. Panel (c) and panel (d) show the location of all 1582
 147 gauging stations in CAMELS-DE; in panel (c) the locations are coloured according to the elevation of the gauging station, while in panel (d) the locations
 148 are coloured according to their mean specific discharge value. borders of Germany: © GeoBasis-DE / BKG (VG250, 2023)

149 3.2 Catchment boundaries derived from MERIT Hydro

150 MERIT (Multi-Error-Removed Improved-Terrain) Hydro was released by Yamazaki et al. (2019); providing a global
 151 hydrography dataset based on the MERIT DEM and various maps of water bodies (e.g. Global 3 arc-second Water Body
 152 Map by Yamazaki et al., 2017). It includes information such as flow direction, flow accumulation, adjusted elevations for
 153 hydrological purposes, and the width of river channels. The delineator.py package (Heberger, 2023) was used to delineate
 154 catchment boundaries. The method automatically derives catchment boundaries from the MERIT Hydro dataset based on the
 155 longitude and latitude of a gauging station and snaps the catchment pour point to the closest stream. Fig. 1b shows all
 156 derived CAMELS-DE catchments using MERIT Hydro within the German borders. The median catchment area within

157 CAMELS-DE is 129.1 km² (Fig. 2a). Compared to other CAMELS datasets, CAMELS-DE includes a large number of
 158 relatively small catchments with an area of less than 100 km² (i.e. 636 catchments, CAMELS-GB: 242 catchments,
 159 CAMELS-US: 142). Uncertainties in catchment delineation arise when comparing areas reported by federal states with those
 160 derived from MERIT Hydro, as shown in Fig. 2b, and these discrepancies are not uniformly distributed across Germany.
 161 They tend to be higher in flat lowland regions with minimal topography (Fig. 2c), particularly in the federal states to the
 162 north and east of Germany. Consequently, a large number of catchments are excluded from the CAMELS-DE dataset in the
 163 northern parts of Germany due to mismatches between reported and estimated areas. In the federal states of Brandenburg
 164 (DE4) and Mecklenburg-Western Pomerania (DE8), for example, we received 447 gauging stations, but given the
 165 uncertainty of the delineation in flat areas, only 277 of them showed a deviation of less than 20 percent from the reported
 166 area. In contrast, in the more mountainous state of Baden-Württemberg (DE1), 225 of 241 catchments met this criterion. As
 167 we report both the catchment areas provided by the federal states and those estimated by MERIT Hydro, the differences
 168 between these two measurements can be used to select or exclude catchments where there are significant uncertainties in the
 169 catchment shape and correspondingly in the derived static and dynamic attributes.



171 **Figure. 2:** Panel (a) shows the distribution of CAMELS-DE catchment areas on a logarithmic scale. Panel (b) shows the accuracy of catchment areas
 172 derived using MERIT Hydro compared to the area reported by the federal agencies; the dashed lines indicate ± 20 percent error tolerance that was set for
 173 catchment selection. Panel (c) shows the absolute relative difference between the reported area by the federal states and the MERIT Hydro area against the
 174 mean catchment elevation. The red line marks the threshold of 20 percent allowed difference for the inclusion of a catchment in the CAMELS-DE dataset.

175 4 Time series

176 CAMELS-DE includes three sets of hydro-meteorological daily time series, as detailed in Table 1, covering the period from
 177 January 1, 1951, to December 31, 2020. These datasets are: (A) observed hydrologic time series (e.g., station discharge and
 178 water levels), (B) observed meteorologic time series (e.g., precipitation, temperature, humidity, and radiation), and
 179 simulated hydro-meteorologic time series (e.g., discharge simulated by a LSTM and a HBV model, including estimated
 180 evapotranspiration). Note that we do not include any information on evaporation in the non-simulated time series data, as we
 181 only include observation-based data here. However, a time series of potential evaporation based on the temperature-based

182 Hargreaves methodology is included in the simulated data (see section 6.2 for more details). However, due to the simplicity
183 of the chosen approach, the potential evapotranspiration time series are highly uncertain, and one should exercise caution
184 when using them.

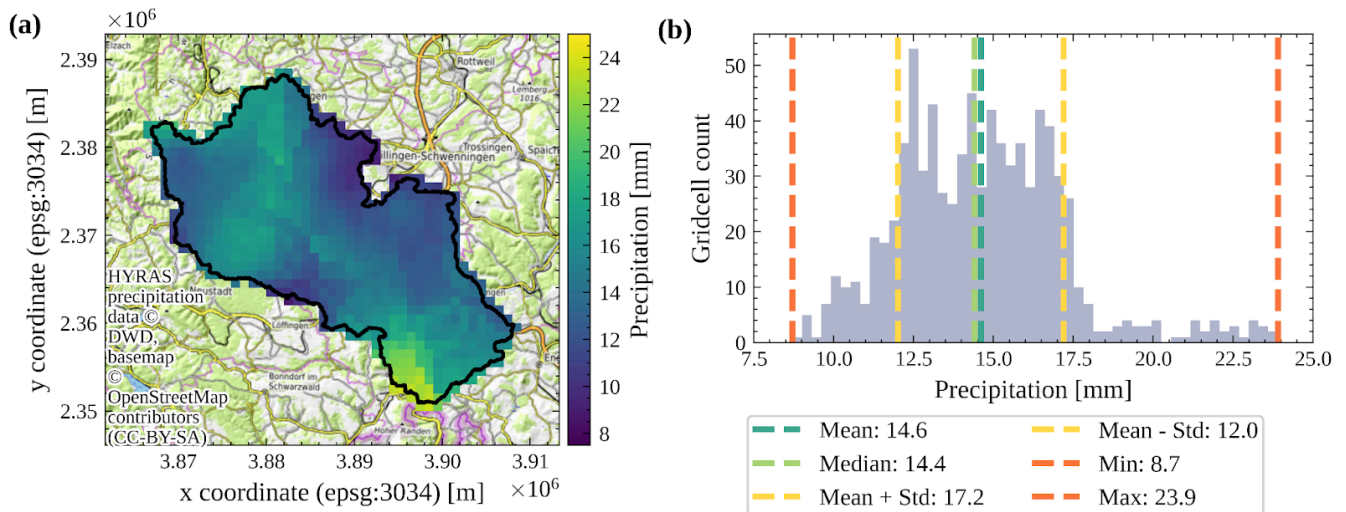
185

186 All meteorological forcing data within CAMELS-DE are sourced from the HYRAS datasets, which are based on the
187 interpolation of meteorological station data (DWD-HYRAS, 2024). This interpolation was conducted by the DWD (see
188 subsection 4.1, 4.2, 4.3). The reliability of these datasets can be compromised by the individual interpolation methods
189 employed (see section 4.1 to 4.3). In addition, inaccuracies in meteorological measurements can introduce uncertainties in
190 the generated grid fields, especially given the extended timescale of 70 years, which may include changes in location and
191 sensor types. Another source of uncertainty is the fact that the number of stations used in the interpolation process varies
192 over time, mirroring changes in the measurement network. For example, the number of stations used for interpolating
193 precipitation data fluctuates, starting at around 4500 in 1951, peaking at approximately 7500 in 2000, and then decreasing to
194 approximately 5000 by 2020. In contrast, the number of stations used for radiation interpolation shows a consistent increase
195 over the years, though the total number remains significantly lower, reaching about 900 stations by 2020. This uncertainty is
196 crucial to consider when comparing data across different years, particularly if the focus is on a single or a few catchments in
197 a certain area. Finally, we use the ‘exact extract’ method, which ensures that raster cells that are only partially covered are
198 treated properly as they are weighted by the proportion of the cell that is covered, i.e. a raster cell that is only 20 % covered
199 by the catchment is only weighted by 20 % when we aggregate to the spatial catchment mean (Fig. 3a illustrates partially
200 covered cells at the catchment boundary). This is particularly important when deriving meteorological data for very small
201 catchment areas. Although this approach also aids in comparing products with different resolutions, it is important to
202 consider that the spatial resolution of the precipitation data, at 1 x 1 km, offers finer detail compared to the 5 x 5 km
203 resolution used for temperature, humidity, and radiation data. This difference is crucial when comparing these datasets within
204 smaller catchments.

205 **4.1 Precipitation**

206 CAMELS-DE utilises precipitation data (mm d^{-1}) with daily resolution, sourced from the HYRAS-DE-PRE dataset v5.0
207 (HYRAS-DE-PRE, 2022). We have calculated daily spatial minimum, mean, median, maximum, and standard deviation of
208 the rainfall field over the catchment for each day. We estimated these statistical measures, rather than just the mean, because
209 this allows us to capture spatial variations and patterns that can be crucial for event characterization or rainfall-runoff
210 modelling, as illustrated in Fig. 3. The HYRAS-DE-PRE dataset v5.0 dataset is produced using the REGNIE interpolation
211 method (Rauhe et al., 2013), which employs daily measured values from meteorological stations to generate an interpolated
212 product on a 1x1 km grid. A detailed description of the interpolation method and the related uncertainties can be found in the
213 official data description (HYRAS-DE-PRE, 2022).

214



215

216 **Figure 3:** Panel (a) shows the catchment boundaries (black line) of the catchment Kirchen-Hausen in Baden-Württemberg overlaid by a clipped daily
 217 precipitation field from the HYRAS dataset on the date 1951-02-20. Panel (b) shows the spatial distribution of rainfall during the same high precipitation
 218 event as (a) over the catchment on 1951-02-20 and the statistical moments (mean, median, standard deviation, minimum and maximum) derived from the
 219 spatial distribution.

220 4.2 Temperature and relative humidity

221 CAMELS-DE employs daily temperature ($^{\circ}\text{C}$) and relative humidity (%), derived from the HYRAS-DE-TAS (daily mean
 222 temperature, HYRAS-DE-TAS, 2022), TASMING (daily minimum temperature, HYRAS-DE-TASMIN, 2022), TASMING
 223 (daily maximum temperature, HYRAS-DE-TASMAX, 2022), and HURS (daily average relative humidity,
 224 HYRAS-DE-HURS, 2022) datasets v5.0, which cover the period from 1951 to 2020 on a 5 km x 5 km grid. This includes the
 225 spatial mean, median, and standard deviation of temperature from HYRAS-DE-TAS, alongside the spatial minimum and
 226 maximum temperatures from TASMING and TASMING, respectively. Additionally, for humidity, we integrate daily minimum,
 227 mean, median, maximum, and standard deviation values across the catchment area. The temperature and humidity data is
 228 based on interpolated station values (Razafimaharo et al., 2020). This interpolation method involves a nonlinear regression at
 229 each time step, aiming to estimate regional vertical temperature profiles across 13 subregions. These subregions are
 230 delineated based on criteria such as weather divides, proximity to the coast, and the extent of north-south variation. A
 231 detailed description of the interpolation method and the related uncertainties can be found in the corresponding data
 232 descriptions (HYRAS-DE-TAS, (2022); HYRAS-DE-TASMIN, (2022); HYRAS-DE-TASMAX, (2022);
 233 HYRAS-DE-HURS, (2022)).

234 4.3 Radiation

235 The CAMELS-DE dataset utilises daily mean global radiation data (in W m^{-2}) derived from the HYRAS-DE-RSDS datasets
 236 v3.0 (HYRAS-DE-RSDS, 2023), that covers a period from 1951 to 2020 with a 5 km x 5 km grid. We have derived daily,

237 spatial minimum, mean, median, maximum, and standard deviation of the radiation field over the catchment for each day.
238 The global radiation (RSDS) dataset integrates station measurement data (including sunshine duration and global radiation),
239 satellite data, and ERA5 data (Muñoz-Sabater et al., 2021). A detailed description of the interpolation method and the related
240 uncertainties can be found in the official data description (HYRAS-DE-RSDS, 2023).

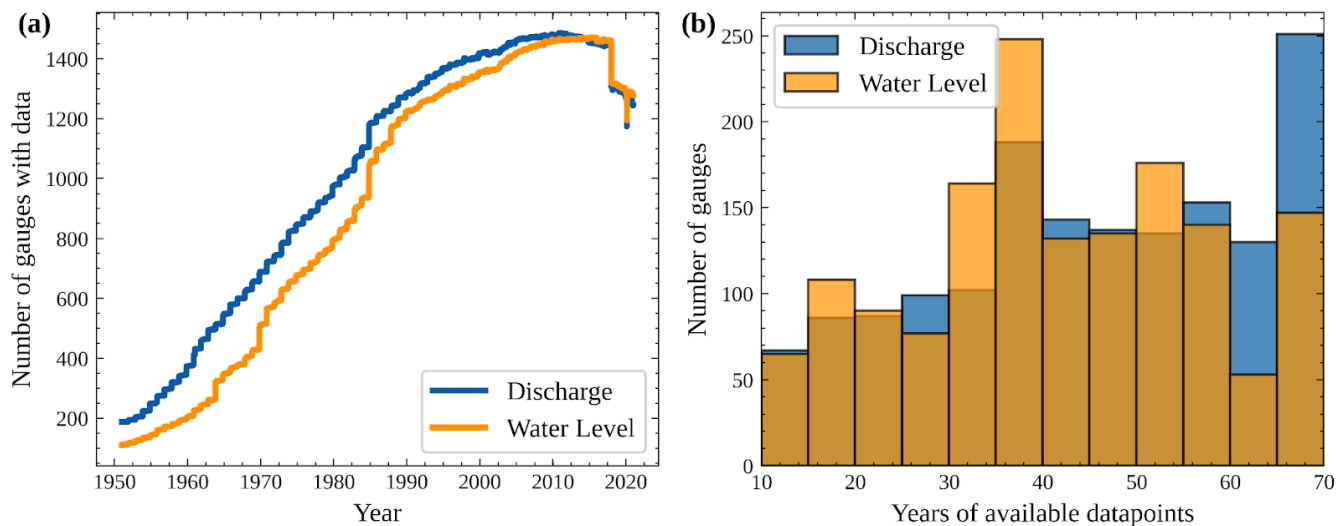
241 **4.4 Discharge and water levels**

242 Observed discharge and water level data were requested from 13 state agencies (see section 2) as time series recorded at the
243 gauging stations (Tab. 1). The number of stations with daily discharge data available per year increases in time from 187 on
244 1 January 1951 to a maximum of 1486 between November 2010 and February 2011 (Fig. 4a). The number of stations with
245 water level data is generally lower, starting at 110 stations on 1 January 1951 and reaching a maximum of 1471 stations
246 between March 2015 and December 2015. The time series span a maximum of 70 years, with each measuring station
247 providing at least 10 years of data between January 1951 and December 2020 (Fig. 4b). These 10 years do not need to be
248 consecutive but typically are. The median time series length of discharge is 46 years, while the median time series length of
249 water level is 40 years. There is a sharp drop-off in Fig. 4a of 137 stations without data from 2017 to 2018 as the provided
250 data from NLWKN (Lower Saxony, DE9) only range until the end of 2017. Another anomaly in Fig. 4a is the drop
251 immediately followed by a rise in the year 2020, which is due to the fact that all measuring stations in Rhineland-Palatinate
252 (DEB) show a gap in the discharge data from 10 February 2020 to 15 February 2020 and in the water level data from 13
253 February 2020 to 15 February 2020. No explanation could be found for this gap. The remaining data after the gap was
254 manually quality controlled by visual inspection of the observed and simulated time series and no reason to exclude this data
255 was found. In total, CAMELS-DE includes 156 stations for which the entire temporal range of 70 years of discharge data is
256 available and for which a maximum of 2 percent of the data is missing in this period. There are 85 stations where this is the
257 case for water level data.

258 **4.5 Discharge and water levels - quality control**

259 The quality control of all discharge and water level data was conducted by the respective federal states (quality controlled
260 data was requested). However, the specific methods employed in this quality control are neither the same across the states,
261 nor are they documented in some cases. Typically, quality control entails that a technical clerk has visually inspected the
262 hydrological time series data. To account for this uncertainty we conducted an additional review of all time series data for
263 high negative values and unrealistically high outliers and replaced such data points with not-a-number (NaN) values. We
264 were conservative in these cases and only deleted values that were clear data errors to not remove potential extreme flood
265 events from the time series. This adjustment was necessary in 8 catchments and is documented in the processing pipeline to
266 assure reproducibility. Please note that negative discharge values are still possible in the CAMELS-DE dataset due to the
267 influence of the tide in the northern part of Germany or due to human influences related to water resources management.
268 Moreover, we assessed the hydro-meteorological time series using both a hydrological model and a data-driven model. This

269 analysis helped us identify catchments with weak correlations between meteorological conditions and hydrological responses
 270 as well as catchments in which the mass balance is far from being closed. All catchments that exhibited a low model
 271 performance of the HBV model were subjected to manual visual inspection, resulting in the removal of 14 catchments (for
 272 more details we refer to section 6).



273

274 **Figure 4:** Panel (a) shows the number of gauging stations with available discharge (blue) and water level data (orange) in the period from 1951 to 2020,
 275 taking into account data gaps, i.e. the data must actually be available at the respective time. Panel (b) shows a histogram of the years of available data points
 276 for all measuring stations, i.e. the length of the time series minus eventual gaps in the time series.

277

278 **Table 1:** Catchment-specific hydro-meteorological variables available as daily time series in CAMELS-DE

| Time series class | Time series name | Description | Unit | Data source |
|--|---|---|----------------------------|--|
| Hydrologic time series (1 Jan 1951–31 Dec 2020) | discharge_vol | Observed catchment discharge calculated from the water level and gauge geometry | $\text{m}^3 \text{s}^{-1}$ | Federal state agencies (see section 2) |
| | discharge_spec | Observed catchment-specific discharge (converted to millimetres per day using catchment areas described in section 3.1) | mm d^{-1} | |
| | water_level | Observed daily water level | m | |
| Meteorologic time series (1 Jan 1951–31 Dec 2020) | precipitation_mean, precipitation_median, precipitation_min, precipitation_max, precipitation_stdev | Observed interpolated spatial mean, median, minimum, maximum and standard deviation of the daily precipitation (original resolution $1 \times 1 \text{ km}^2$) | mm d^{-1} | German Weather Service HYRAS (DWD-HYRAS, 2024) |
| | temperature_min | Observed interpolated spatial mean daily minimum temperatures (original resolution $5 \times 5 \text{ km}^2$) | $^{\circ}\text{C}$ | |
| | temperature_mean | Observed interpolated spatial mean daily mean | $^{\circ}\text{C}$ | |

| | | | | |
|---|--|--|--------------------------------|--|
| | | temperatures (original resolution 5x5 km ²) | | |
| | temperature_max | Observed interpolated spatial mean daily maximum temperatures (original resolution 5x5 km ²) | °C | |
| | humidity_mean, humidity_median, humidity_min, humidity_max, humidity_stdev | Observed interpolated spatial mean, median, minimum, maximum and standard deviation of the daily humidity (original resolution 5x5 km ²) | % | |
| | radiation_global_mean, radiation_global_median, radiation_global_min, radiation_global_max, radiation_global_stdev | Observed interpolated spatial mean, median, minimum, maximum and standard deviation of the global radiation (original resolution 5x5 km ²) | W m ² | |
| Simulated hydrologic time series (1 Jan 1951–31 Dec 2020) | pet_hargreaves | Daily mean of potential evapotranspiration calculated using the Hargreaves equation | mm d ⁻¹ | Regional LSTM model, HBV model and Hargreaves equation for potential evapotranspiration (see section 6, https://github.com/KIT-HYD/Hy2DL/tree/v1.1 , last access: 24 July 2024) |
| | discharge_vol_obs | Observed volumetric discharge | m ³ s ⁻¹ | |
| | discharge_spec_obs | Observed catchment-specific discharge | mm d ⁻¹ | |
| | discharge_vol_sim_lstm | Volumetric discharge calculated from discharge_spec_sim_lstm and the catchment area | m ³ s ⁻¹ | |
| | discharge_spec_sim_lstm | Catchment-specific discharge simulated with the LSTM (see section 6) | mm d ⁻¹ | |
| | discharge_vol_sim_hbv | Volumetric discharge calculated from discharge_spec_sim_hbv and the catchment area | m ³ s ⁻¹ | |
| | discharge_spec_sim_hbv | Catchment-specific discharge simulated with the HBV model (see section 6) | mm d ⁻¹ | |
| | simulation_period (training, validation, testing) | Flag indicating the simulation period in which the daily value is contained (training, validation, testing) | – | |

279 5 Catchment attributes

280 In addition to the daily time series of hydro-meteorological variables available in CAMELS-DE, the dataset also includes a
281 series of static catchment attributes which are considered time-invariant and include information about topography (section
282 5.1), hydroclimatic signatures (section 5.2) and catchment attributes covering land-cover (section 5.3), soil (section 5.4),
283 hydrogeology (section 5.5) and human influences (section 5.6).

284 5.1 Location and topography

285 For CAMELS-DE, we developed a system of catchment IDs, since the official IDs used by the federal states are inconsistent
286 beyond federal state boundaries. However, the official provider IDs are contained in the topographic attributes of the dataset

287 (Tab. 2). The gauge IDs in CAMELS-DE are based on the NUTS classification, which divides the EU territory hierarchically
288 according to administrative boundaries. In Germany, the first hierarchical level NUTS 1 provides a code for each federal
289 state (e.g. DE7 for Hessen, DED for Saxony; Fig. 1b). We assign an ID code to each gauge as follows. The ID of each gauge
290 starts with the NUTS 1 code of the corresponding federal state. For each federal state the gauges are coded in arbitrary order
291 starting from 10000 for the first gauge and adding a step of 10 for each following gauge (e.g. DE710000 for the first station
292 in Hessen, DE710010 for the second station, DE710020 for the third station, etc.). This system ensures consistency of the
293 gauge IDs in Germany, and additionally provides the information about the federal state of each gauge. Topographic
294 attributes such as the location (coordinate systems WGS84 and ETRS89), gauge elevation (m) and catchment area (km²)
295 were provided by the federal agencies, the area of the MERIT Hydro catchment is also provided. Additionally we derived the
296 gauge point elevation (m) and basic statistical variables (min, mean, median, 5th and 95th percentile, max) of the catchment
297 elevation (m) from the GLO-30 DEM. CAMELS-DE additionally provides the location of all gauging stations and catchment
298 boundaries as a shape file and a geopackage file.

299 5.2 Climate and hydrology

300 For the CAMELS-DE dataset, we calculated long-term climatic and hydrological signatures in line with the attributes found
301 in CAMELS-CH (covering the period between 1981–2020) and CAMELS-UK (covering the period between 1970–2015)
302 with the difference that we cover the period from 1951–2021 (see Tab. 2). Both types of attributes are calculated based solely
303 on complete hydrological years with respect to the discharge (1 October to 30 September of the following year; again inline
304 with the definition of a hydrological year chosen in CAMELS-UK and CAMELS-CH), with a maximum tolerance of 5 %
305 missing values per hydrological year, ensuring robustness in the data used for analysis. If a specific catchment has discharge
306 data for only a limited number of hydrologic years, we calculate the climatic and hydrological indices for those same years to
307 maintain consistency across all CAMELS datasets and across the climatic and hydrological attributes.

308

309 For each catchment, the hydrologic attributes include values for the mean specific discharge (mm d⁻¹), the runoff ratio, the
310 start and end dates of available discharge data, the percentage of days on which discharge data is available (%), the slope of
311 the flow duration curve between the log-transformed 33rd and 66th percentiles, the number of days after which the
312 cumulative discharge since 1 October reaches half of the annual discharge (d), the 5th and 95th quantile of specific discharge
313 (mm d⁻¹) and the frequency of high flow, low flow and zero flow days (d yr⁻¹) together with the average duration of high-flow
314 and low-flow events (d). The climatic attributes are calculated on the basis of the HYRAS meteorological data for each
315 catchment and include mean daily precipitation (mm d⁻¹), the seasonality of precipitation, the fraction of precipitation falling
316 as snow, the frequency of high and low precipitation days (d yr⁻¹), the average duration of high precipitation events and dry
317 periods (d) as well as the season during which most high and low precipitation days occur. The code to estimate the
318 signatures in CAMELS-DE is based on the codes used to derive the signatures for CAMELS-US
319 (<https://github.com/naddor/camels>, last access: 19 July 2024), CAMELS-UK and CAMELS-CH to assure compatibility.

320 **5.3 Land cover**

321 Land cover in CAMELS-DE is derived from the Corine Land Cover dataset (CLC, 2018) which provides consistent and
322 thematically detailed information on land cover across Europe. The dataset was produced within the frame of the Copernicus
323 Land Monitoring Service referring to land cover / land use status of the year 2018 and is based on the classification of
324 satellite images (other major releases have been published in the years 1990, 2000, 2006, 2012). The CLC dataset from 2018
325 has a spatial resolution of 100 m for raster data. This ensures detailed and consistent land cover information across Europe.
326 CAMELS-DE includes land cover percentages per catchment of the first hierarchical land cover level: artificial surfaces,
327 agricultural areas, forests and semi-natural areas, wetlands and water bodies. The decision to not mix the hierarchical land
328 cover levels ensures that uncertainties in classification due to varying levels of detail are minimised. Catchment shapes and
329 codes to derive land cover classes of lower order or from different releases of CLC in a consistent manner with
330 CAMELS-DE are delivered with the dataset (Dolich, 2024).

331 **5.4 Soil**

332 Soil attributes for CAMELS-DE are derived from the SoilGrids250m dataset (Poggio et al., 2021), which maps the spatial
333 distribution of soil properties globally at six standard depths. The SoilGrids dataset is generated by training a machine
334 learning model on approximately 240,000 locations worldwide, using over 400 global environmental covariates that describe
335 vegetation, terrain morphology, climate, geology, and hydrology. For CAMELS-DE, we derived the mean values of the soil
336 bulk density, soil organic carbon, volumetric percentage of coarse fragments and proportions of clay, silt and sand for each
337 catchment. The resulting variables are aggregated from the six SoilGrid depths to the depths 0-30 cm, 30-100 cm and
338 100-200 cm by calculating a weighted mean. The accuracy of soil property models, as described by Poggio et al. (2021), is
339 limited by the availability and quality of input data and the assumptions in the modelling process. For instance, discrepancies
340 in how soil data are collected, analysed, and reported by different entities challenge efforts toward data standardisation and
341 harmonisation. However, the relatively high number of observations in Germany reduces this uncertainty to a certain extent.
342 Furthermore, the defined catchment boundaries allow for an assessment of the reported uncertainties within each catchment.
343 If needed the catchment boundaries delivered with CAMELS-DE can be used to calculate the reported uncertainties of
344 SoilGrids within each catchment.

345 **5.5 Hydrogeology**

346 The hydrogeological attributes for CAMELS-DE are derived from the hydrogeological overview map of Germany on the
347 scale of 1:250,000; "HÜK250" (HGM250, 2019), which describes the hydrogeological characteristics of the upper,
348 large-scale contiguous aquifers in Germany. For CAMELS-DE, the areal percentage of the various HÜK250 classes (see
349 Tab. 2) was calculated for each catchment, whereby the variables of the classes permeability, aquifer media type, cavity type,
350 consolidation, rock type and geochemical rock type sum to 100 percent. Uncertainties in these data may arise from the

351 generalisation required to scale point measurements to a gridded product, which can oversimplify complex hydrogeological
352 features, potentially leading to inaccuracies in the representation of local variations and the spatial distribution of aquifer
353 properties.

354 **5.6 Human influence**

355 CAMELS-DE includes information on human influences within catchments, primarily focusing on existing dams and
356 reservoirs in Germany. This information is sourced from the inventory of dams in Germany (Speckhann et al., 2021), which
357 offers detailed data including dam names, locations, associated rivers, years of construction and operation start, crest lengths,
358 dam heights, lake areas, lake volumes, purposes (such as flood control or water supply), dam structure types, and specific
359 building characteristics for 530 dams across Germany. For catchments containing multiple dams, this data is aggregated to
360 provide a comprehensive overview. Specifically, CAMELS-DE includes key information about the dams within each
361 catchment, such as the number of dams, the names of the dams, the rivers where these dams are located, the operational
362 years of the oldest and newest dams, the total area and volume of all dam lakes at full capacity, and the overall purposes of
363 these dams. It is important to note that the “Inventory of Dams in Germany” does not claim to be exhaustive. The absence of
364 recorded dams in this inventory does not necessarily indicate a lack of human influence within a catchment. Nearly all
365 catchments in Germany experience substantial anthropogenic influences, and it is likely that some dams, weirs, or reservoirs
366 (particularly smaller ones) are not documented in the dataset. Another relevant indicator of human influence included in
367 CAMELS-DE is hence the proportion of artificial and agricultural surfaces derived from land cover attributes (see section
368 5.3).

369 **6 Benchmark LSTM and HBV model**

370 CAMELS-DE, in addition to hydro-meteorological observations and catchment attributes, includes results from data-driven
371 and conceptual lumped rainfall-runoff simulations for each catchment. More specifically, these results are derived from a
372 regionally trained LSTM network (trained on all catchments at the same time) and a locally trained lumped HBV model
373 (trained at each individual catchment; Bergström and Forsman, 1973, Seibert, 2005, Feng et al., 2022). These models serve
374 three main purposes: (a) they are used to identify catchments where the relationship between meteorological forcing and
375 streamflow is difficult to capture (low model performance), indicating possible strong human influences such as dams or
376 reservoirs, or potential issues with the catchment delineation or the streamflow or meteorological time series; (b) they can
377 serve as a benchmark for future modelling studies based on CAMELS-DE in a sense that the reported performance values
378 and time series can be used as a baseline model and (c) in case of a good model performance can be used to fill missing
379 values of the observed discharge time series. Both models were trained over the period from October 1, 1970, to December
380 31, 1999, validated from October 1, 1965, to September 30, 1970, and tested from January 1, 2000, to December 31, 2020.
381 CAMELS-DE includes the simulated discharges for both models for the entire 70 years (Tab. 1), a flag was added to indicate

382 if the corresponding time step was used in training, validation or testing. In the following we explain the model setups and
383 analyse the simulation results in detail. The code of the LSTM model and the HBV model were carefully tested and
384 benchmarked (Acuña Espinoza et al., 2024). The codes have been designed to allow easy access and a permalink to the code
385 version used for CAMELS-DE can be found here (<https://github.com/KIT-HYD/Hy2DL/tree/v1.1>, last access: 24 July 2024).

386 6.1 Setup LSTM model

387 The LSTM uses mean precipitation, standard deviation of precipitation, mean radiation, mean minimum temperature and
388 mean maximum temperature as dynamic (time varying) input features and specific discharge as a target variable. Static
389 features and hyperparameters were set according to the study of Acuña et al. (2024) with modifications made to (1) an
390 increased hidden size from 64 to 128 and (2) a reduced number of epochs from 30 to 20. The remaining hyperparameters
391 were set as follows: number of hidden layers = 1; learning rate = 0.001; dropout rate = 0.4; batch size = 256; sequence length
392 = 365 days; iterative optimization algorithm = Adam. We use the basin-averaged Nash-Sutcliffe Efficiency (NSE*) loss
393 function proposed by Kratzert et al. (2019) to avoid an imbalance during training due to the higher influence of catchments
394 with a higher runoff generation. In addition, to the model results (see Tab. 2), we provide the model training epochs of the
395 regional LSTM as part of the CAMELS-DE dataset.

396 6.2 Setup HBV model

397 The lumped HBV model used in CAMELS-DE is a variant of the well-known HBV (Hydrologiska Byråns
398 Vattenbalansavdelning; Bergström and Forsman, 1973) model. A detailed description of the model architecture and setup can
399 be found in the studies by Seibert (2005) and Feng et al. (2022). HBV uses mean precipitation and potential
400 evapotranspiration (E_{pot} ; mm d^{-1}) as inputs. The E_{pot} is calculated using the temperature-based Hargreaves formula, detailed
401 by Adam et al. (2006) and based on earlier work by Droogers and Allen (2002), as explained and cited in
402 Clerc-Schwarzenbach et al. (2024). This variant of the Hargreaves formula resulted in the lowest mass balance error in most
403 catchments with respect to other methods (e.g. Penman, Priestly Taylor) to estimate evapotranspiration and was additionally
404 chosen due to its low data requirements, enabling the utilisation of HYRAS precipitation and temperature data to generate
405 the E_{pot} time series with a limited number of assumptions. The E_{pot} time series are included in CAMELS-DE (Tab. 2) for the
406 entire time period of 70 years. In terms of model calibration, the SHM was trained individually for each basin using the NSE
407 as a loss function, employing the Differential Evolution Adaptive Metropolis (DREAM; Vrugt, 2016) algorithm as
408 implemented in the SPOTPY (SPOTting model parameters using a ready-made PYthon package, Houska et al., 2015)
409 library. In contrast to the LSTM, the SHM model is mass conserving and hence more sensitive to errors in the catchment
410 delineation that can lead to mass balance errors (see section 3). The difference between the SHM and the LSTM performance
411 can be seen as an indicator either for a strong human influence or for an imprecise catchment delineation as the LSTM can
412 create mass. In addition to the model results (see Tab. 2), we provide the HBV model parameters for each catchment as part
413 of the CAMELS-DE dataset.

414 6.3 Results LSTM and SHM model

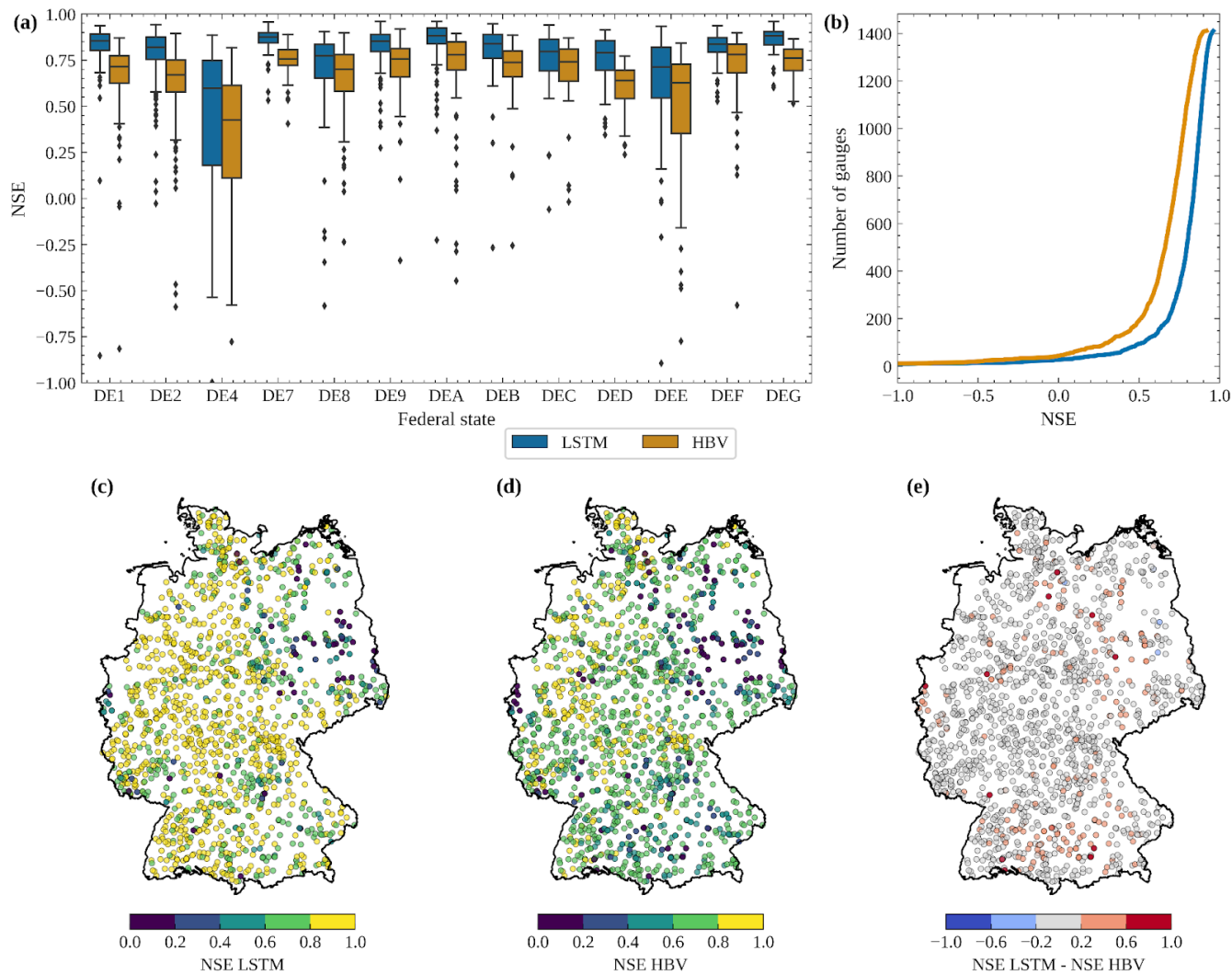
415 In this section, we focus our analysis on the LSTM and SHM model in catchments where at least 20 % of the daily data is
416 available during the 30-year training period and 10 % during the testing period, covering a total of 1411 catchments. The
417 median performance of the LSTM, as quantified by the NSE during the testing period, is 0.84 across 1411 catchments. Of
418 these, 94 catchments have an NSE lower than 0.5 (6.66 % of all catchments), out of which 28 have a negative NSE (1.98 %
419 of all catchments). For the 94 catchments with NSE below 0.5, most streamflow time series exhibit a low Pearson correlation
420 with daily precipitation (< 0.1) and these catchments are often considerably affected by the construction and/or operation of
421 dams or flood control structures (human influences attributes). Therefore, model performance of the LSTM network can be
422 used to identify catchments that are subject to considerable uncertainties, either due to measurement inaccuracies or
423 significant human influences.

424

425 Fig. 5a illustrates the performance of the LSTM model across various federal states, with relatively consistent results across
426 the board except for the federal states of Brandenburg (DE4) and Saxony-Anhalt (DEE). In Brandenburg, lowland
427 catchments characterised by sandy soils, considerable groundwater impacts, abundance of natural lakes and human
428 constructed weirs, canals and cross-connections between streams most likely yield a distinctly lower model performance
429 compared to the rest of the German federal states. Besides the federal state of Brandenburg and Saxony-Anhalt the analysis
430 of the LSTMs simulations reveals no clear correlation between the model performance and the topographic attributes (e.g.,
431 area), climatic attributes (e.g., long-term mean precipitation), or hydrological attributes (e.g., long-term mean flow).

432

433 The performance of HBV is with a median NSE of 0.72 lower than that of the LSTM (Fig. 5b). In 192 catchments (13.61 %)
434 the HBV shows a performance below a NSE of 0.5 and in 44 (3.12 %) a performance below a NSE of 0. The spatial patterns
435 of performance measured by the NSE are consistent between the LSTM and HBV. In other words, catchments where the
436 LSTM performs well are typically also accurately represented by HBV, and vice versa, as illustrated in Fig. 5e. Catchments
437 in which HBV significantly underperforms compared to the LSTM are almost invariably strongly influenced by
438 human-made structures such as dams or weirs, or they are located in areas with uncertain catchment delineation. We propose
439 that the HBV model, which conserves mass and uses time-invariant parameters, struggles to adapt to dynamic changes in
440 catchment function caused by human activities that result in inaccuracies in water flow and storage due to structures like
441 dams, weirs or due to irrigation or pumping. A hypothesis that requires further testing in the few catchments where this is the
442 case.



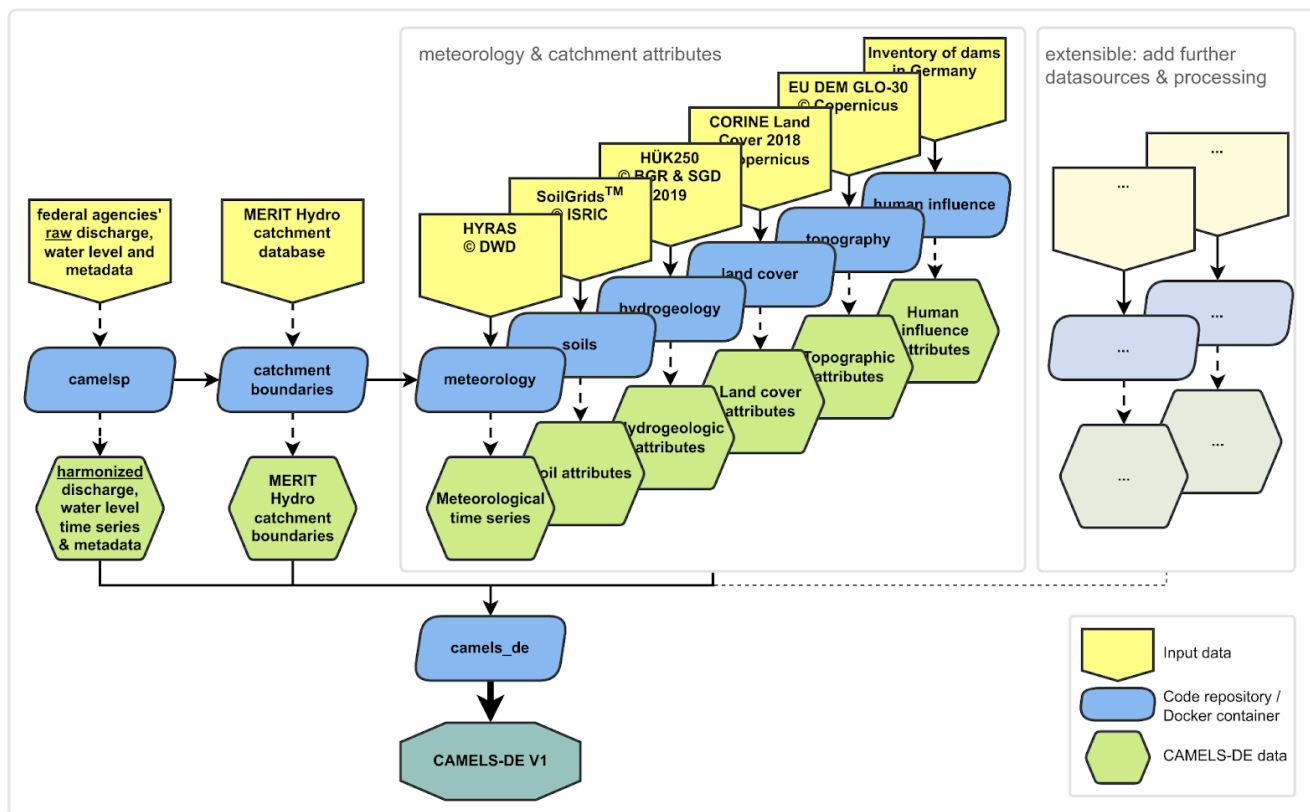
443

444 **Figure 5:** Panel (a) shows boxplots visualising the distribution of the NSE of the LSTM network (blue) and the HBV model (orange) for each federal state
 445 in Germany for the testing period. Panel (b) shows a cumulative plot of the NSE for the general comparison of the LSTM model and the HBV model. Panel
 446 (c) shows the NSE values of the LSTM for 1411 gauging stations in Germany, while panel (c) shows the same for the NSE values of the HBV model. Panel
 447 (e) shows the difference between the NSE values of the LSTM and the HBV model for all gauging stations in Germany, borders of Germany: ©
 448 GeoBasis-DE / BKG (VG250, 2023)

449 7 Code availability, reproducibility and extensions

450 The processing of CAMELS-DE is structured in a modular manner to enhance the clarity and reproducibility of the
 451 processing pipeline. The CAMELS-DE processing pipeline was published separately with more details and permalinks to the
 452 released repository versions that represent the code state that was used to process and compile CAMELS-DE (Dolich, 2024).

453 For each component of CAMELS-DE, a distinct GitHub repository was established. Within each repository, a dedicated
454 Docker container was developed to process specific input datasets (e.g. HYRAS, GLO-30 DEM). Containerization is
455 particularly well-suited for this project as it ensures that each component of the data processing pipeline runs consistently
456 across different computing environments. This containerization simplifies dependency management, enhances
457 reproducibility, and facilitates the deployment and version control of each processing module. Fig. 6 illustrates the
458 architecture of the processing pipeline, where each blue block represents an individual GitHub repository equipped with a
459 Docker container that processes the yellow input data to produce the green output data. All repositories are uniformly
460 structured, and the accompanying documentation provides detailed descriptions of each repository, guidelines for building
461 and running the Docker containers, including the necessary folder mounts, and instructions for accessing the required input
462 data. In the initial phase of the CAMELS-DE data processing pipeline, raw discharge and water level data, along with station
463 metadata provided by the federal states, are processed and harmonised. Subsequently, MERIT-Hydro catchment boundaries
464 are delineated for each station, a pivotal step since all further datasets depend extensively on these catchment boundaries.
465 Meteorological time series data for these catchments are then processed to compute statistics such as area mean and median.
466 Following this, attributes such as soil properties, hydrogeology, land cover, topography, and human influences are derived for
467 each catchment (see Table 2). In the final stage, all derived data are integrated and formatted according to the established
468 structure of the CAMELS-DE dataset, mirroring the organisational schema of CAMELS-GB or CAMELS-CH.



469

470 **Figure 6:** Diagram of the CAMELS-DE data processing pipeline. Starting with raw discharge and metadata harmonisation, it proceeds to derive
 471 MERIT-Hydro catchment boundaries. Subsequent processing includes meteorological data extraction and aggregation followed by the extraction of various
 472 catchment attributes. In the final step, all extracted data sources are integrated in the structured CAMELS-DE dataset, consistent with CAMELS-GB or
 473 CAMELS-CH (Dolich, 2024).

474 The modular design of the CAMELS-DE processing pipeline enhances its traceability, comprehensibility, and
 475 reproducibility, differing significantly from a monolithic code approach that compiles the entire dataset into a single
 476 repository. This structure not only facilitates the extension of the pipeline to incorporate additional data sources, especially
 477 further catchment attributes, without the need to re-run or rewrite the entire system but also allows for the adaptation of
 478 processing or aggregation methods and the seamless release of updated versions of the CAMELS-DE dataset. The publicly
 479 available Docker containers and the code within them serve not only as a comprehensive guide to understanding the data
 480 processing methods used in CAMELS-DE but also provide a foundation for further data processing using the catchment
 481 geometries included in the dataset. We encourage researchers to enrich CAMELS-DE with additional data sources and
 482 explore ways to enhance the baseline model results. Such contributions are invaluable for continuous improvements and
 483 expansions of the CAMELS-DE dataset, reflecting our commitment to advancing hydrological research and applications
 484 through reproducible science.

485 8 Data availability

486 This manuscript describes the state of version 1.0 of CAMELS-DE, which is freely available at
487 <https://doi.org/10.5281/zenodo.13837553> (Dolich et al., 2024), accompanied by a comprehensive data description. The code
488 to reproduce CAMELS-DE can be found at <https://doi.org/10.5281/zenodo.12760336> (Dolich, 2024).

489 9 Conclusions

490 CAMELS-DE is a significant step forward in hydrological research for Germany and beyond, offering a comprehensive
491 dataset that spans 1582 catchments with hydro-meteorological daily time series from 1951 to 2020. CAMELS-DE includes
492 detailed catchment delineations and properties, such as reservoir data, land-use, soils, and hydrogeology, which are all vital
493 to analyse and describe the local and regional hydrology of Germany. Furthermore, CAMELS-DE includes simulations from
494 a regionally trained LSTM and locally trained HBV model that can be used either to fill gaps in discharge data in case of
495 good model performance or act as baseline models for the development and testing of new hydrological models. Due to the
496 length of the provided time series of up to 70 years CAMELS-DE opens up new opportunities for investigating long-term
497 hydrological trends or conducting large-sample studies across diverse catchments, including a large number of catchments
498 smaller than 100 km². The dataset's modular design, achieved through the containerization of each processing component,
499 ensures that the data processing is traceable, comprehensible, and reproducible. This approach makes it easier to extend the
500 dataset by incorporating new data sources, adapting processing methods, and releasing updated versions without the need to
501 re-run the entire pipeline. While CAMELS-DE serves as a useful benchmark for large sample hydrology, we invite the
502 scientific community to enrich it with additional data sources and improved methods. In conclusion, CAMELS-DE aims to
503 support a broad range of hydrological research and applications, to foster better understanding and management of water
504 resources in Germany and beyond and to contribute to future global hydrological studies.

505

506 **Author contribution:** RL and MS initiated the CAMELS-DE project. AD prepared and processed data, created most figures
507 and wrote together with RL most of the manuscript. All other authors suggested improvements and made additions to the
508 manuscript, as well as provided data and expertise for specific topics.

509

510 **Competing interests:** At least one of the (co-)authors is a member of the editorial board of Earth System Science Data or
511 Hydrology and Earth System Sciences.

512

513 **Acknowledgment:** We thank the various German institutions for providing observation-based data and sharing their
514 expertise. We are grateful to the Volkswagen Foundation for funding the “CAMELS-DE” project within the framework of

515 the project "Invigorating Hydrological Science and Teaching: Merging Key Legacies with New Concepts and Paradigms"
 516 (ViTamins). We also extend our thanks to NFDI4Earth, particularly Jörg Seegert, for their support and suggestions.
 517

518 **Table 2.:** Catchment-specific static attributes available in CAMELS-DE

| Attribute class | Attribute name | Description | Unit | Data source |
|-------------------------|---|--|-----------------|--|
| Location and topography | gauge_id | catchment identifier based on the NUTS classification as described in section 5.1 e.g. DE110000, DE110010, ... | – | Federal state agencies (see section 2) |
| | provider_id | official gauging station ID assigned by the federal states | – | |
| | gauge_name | gauging station name | | |
| | water_body_name | water body name | – | |
| | federal_state | federal state in which the measuring station is located | | |
| | gauge_lon | gauging station longitude (EPSG:4326) | ° | |
| | gauge_lat | gauging station latitude (EPSG:4326) | ° | |
| | gauge_easting | gauging station easting (EPSG:3035) | m | |
| | gauge_northing | gauging station northing (EPSG:3035) | m | |
| | gauge_elev_metadata | gauging station elevation as given by the federal states | m a.s.l. | |
| area_metadata | catchment area as given by the federal states | km ² | | |
| | gauge_elev | gauging station elevation derived from the GLO-30 DEM | m a.s.l. | Copernicus GLO-30 DEM (EU-DEM, 2022) |
| | area | catchment area derived from the MERIT Hydro catchment | km ² | |
| | elev_mean | mean elevation in the catchment based on the MERIT Hydro geometry | m a.s.l. | |
| | elev_min | minimum elevation within catchment | m a.s.l. | |
| | elev_5 | 5th percentile elevation within catchment | m a.s.l. | |
| | elev_50 | median elevation within catchment | m a.s.l. | |
| | elev_95 | 95th percentile elevation within catchment | m a.s.l. | |

| | | | | |
|-----------|--------------------|---|--------------------|---|
| | elev_max | maximum elevation within catchment | m a.s.l. | |
| Climate | p_mean | long-term mean of daily precipitation from 1951 to 2020 | mm d ⁻¹ | German Weather Service HYRAS (DWD-HYRAS, 2024) |
| | p_seasonality | seasonality and timing of precipitation (estimated using sine curves to represent the annual temperature and precipitation cycles, positive (negative) values indicate that precipitation peaks in summer (winter), and values close to zero indicate uniform precipitation throughout the year). | – | |
| | frac_snow | fraction of precipitation falling as snow, i.e. while mean air temperature is < 0° C | – | |
| | high_prec_freq | frequency of high-precipitation days (≥ 5 times mean daily precipitation) | d yr ⁻¹ | |
| | high_prec_dur | mean duration of high-precipitation events (number of consecutive days ≥ 5 times mean daily precipitation) | d | |
| | high_prec_timing | season during which most high-precipitation days occur, e.g. 'jja' for summer. If two seasons register the same number of events a value of NA is given. | season | |
| | low_prec_freq | frequency of dry days (< 1 mm d ⁻¹) | d yr ⁻¹ | |
| | low_prec_dur | mean duration of dry periods (number of consecutive days < 1 mm d ⁻¹ mean daily precipitation) | d | |
| | low_prec_timing | season during which most dry season days occur, e.g. 'son' for autumn. If two seasons register the same number of events a value of NA is given. | season | |
| Hydrology | q_mean | mean daily specific discharge | mm d ⁻¹ | Federal state agencies (see section 3.1) and German Weather Service HYRAS (DWD-HYRAS, 2024) |
| | runoff_ratio | runoff ratio (ratio of mean daily discharge to mean daily precipitation) | – | |
| | flow_period_start | first date for which daily streamflow data is available | – | |
| | flow_period_end | last day for which daily streamflow data is available | – | |
| | flow_perc_complete | percentage of days for which streamflow data is available from Jan 1951–31 Dec 2020 | % | |
| | slope_fdc | slope of the flow duration curve (between the log-transformed 33rd and 66th stream flow percentiles, see Coxon et al. (2020)) | – | |
| | hfd_mean | mean half-flow date (number of days since 1. | d | |

| | | | | |
|------------|--|--|--------------------|-------------------------------------|
| | | Oct at which the cumulative discharge reaches half of the annual discharge) | | |
| | Q5 | 5 % flow quantile (low flow) | mm d ⁻¹ | |
| | Q95 | 95 % flow quantile (high flow) | mm d ⁻¹ | |
| | high_q_freq | frequency of high-flow days (> 9 times the median daily flow) | d yr ⁻¹ | |
| | high_q_dur | mean duration of high-flow events (number of consecutive days > 9 times the median daily flow) | d | |
| | low_q_freq | frequency of low-flow days (< 0.2 times the mean daily flow) | d yr ⁻¹ | |
| | low_q_dur | mean duration of low-flow events (number of consecutive days < 0.2 times the mean daily flow) | d | |
| | zero_q_freq | fraction of days with zero stream flow | – | |
| Land cover | artificial_surfaces_perc | areal coverage of artificial surfaces | % | CORINE Land Cover 2018 (CLC, 2018) |
| | agricultural_areas_perc | areal coverage of agricultural areas | % | |
| | forests_and_seminatural_areas_perc | areal coverage of forests and semi-natural areas | % | |
| | wetlands_perc | areal coverage of wetlands | % | |
| | water_bodies_perc | areal coverage of water bodies | % | |
| Soil | clay_0_30cm_mean clay_30_100cm_mean clay_100_200cm_mean | weight percent of clay particles (< 0.002 mm) in the fine earth fraction at depths 0 - 30 cm, 30 - 100 cm and 100 - 200 cm | wt. % | SoilGrids250m (Poggio et al., 2021) |
| | silt_0_30cm_mean silt_30_100cm_mean silt_100_200cm_mean | weight percent of silt particles (≥ 0.002 mm and ≤ 0.05/0.063 mm) in the fine earth fraction at depths 0 - 30 cm, 30 - 100 cm and 100 - 200 cm | wt. % | |
| | sand_0_30cm_mean sand_30_100cm_mean sand_100_200cm_mean | weight percent of sand particles (> 0.05/0.063 mm) at depths 0 - 30 cm, 30 - 100 cm and 100 - 200 cm | wt. % | |
| | coarse_fragments_0_30cm_mean coarse_fragments_30_100cm_mean coarse_fragments_100_200cm_mean | volumetric fraction of coarse fragments (> 2 mm) at depths 0 - 30 cm, 30 - 100 cm and 100 - 200 cm | vol % | |
| | soil_organic_carbon_0_30cm_mean soil_organic_carbon_30_100cm_mean soil_organic_carbon_100_200cm_mean | soil organic carbon content in the fine earth fraction at depths 0 - 30 cm, 30 - 100 cm and 100 - 200 cm | g kg ⁻¹ | |

| | | | | |
|--------------|--|--|---------------------|---|
| | bulk_density_0_30cm_mean bulk_density_30_100cm_mean bulk_density_100_200cm_mean | bulk density of the fine earth fraction at depths 0 - 30 cm, 30 - 100 cm and 100 - 200 cm | kg dm ⁻³ | |
| Hydrogeology | aquitard_perc aquifer_perc aquifer_aquitard_mixed_perc | areal coverage of aquifer media type classes | % | HÜK250 © BGR & SGD (Staatlichen Geologischen Dienste) 2019 (HGM, 2019) |
| | kf_very_high_perc (>1E-2 m s ⁻¹) kf_high_perc (>1E-3 – 1E-2 m s ⁻¹) kf_medium_perc (>1E-4 – 1E-3 m s ⁻¹) kf_moderate_perc ((>1E-5 – 1E-4 m s ⁻¹) kf_low_perc (>1E-7 – 1E-5 m s ⁻¹) kf_very_low_perc (>1E-9 - 1E-7 m s ⁻¹) kf_extremely_low_perc (<1E-9 m s ⁻¹) kf_very_high_to_high_perc (>1E-3 m s ⁻¹) kf_medium_to_moderate_perc (>1E-5 – 1E-3 m s ⁻¹) kf_low_to_extremely_low_perc (<1E-5 m s ⁻¹) kf_highly_variable_perc kf_moderate_to_low_perc (>1E-6 – 1E-4 m s ⁻¹) | areal coverage of permeability classes | % | |
| | cavity_fissure_perc cavity_pores_perc cavity_fissure_karst_perc cavity_fissure_pores_perc | areal coverage of cavity type classes | % | |
| | consolidation_solid_rock_perc consolidation_unconsolidated_rock_perc | areal coverage of consolidation classes | % | |
| | rocktype_sediment_perc rocktype_metamorphite_perc rocktype_magmatite_perc | areal coverage of rock type classes | % | |
| | geochemical_rocktype_silicate_perc geochemical_rocktype_silicate_carbonatic_perc geochemical_rocktype_carbonatic_perc geochemical_rocktype_sulfatic_perc geochemical_rocktype_silicate_organic_components_perc geochemical_rocktype_anthropogenically_modified_through_filling_perc geochemical_rocktype_sulfatic_halitic_perc geochemical_rocktype_halitic_perc | areal coverage of geochemical rock type classes | % | |

c

| | | | | |
|--------------------------|--------------------------|--|--------------------|---|
| | waterbody_perc | areal coverage of water body areas according to hydrogeological map | % | |
| | no_data_perc | percentage of areas with missing data | % | |
| Human influence | dams_names | names of all dams located in the catchment | – | Inventory of dams in Germany (Speckhann et al., 2021) |
| | dams_river_names | names of the rivers where the dams are located | – | |
| | dams_num | number of dams located in the catchment | – | |
| | dams_year_first | year when the first dam entered operation | – | |
| | dams_year_last | year when the last dam entered operation | – | |
| | dams_total_lake_area | total area of all dam lakes at full capacity | km ² | |
| | dams_total_lake_volume | total volume of all dam lakes at full capacity | Mio m ³ | |
| | dams_purposes | purposes of all the dams in the catchment | – | |
| Hydrological Simulations | training_perc_complete | percentage of observed specific discharge values in the training period (1970-10-01 – 1999-12-31) that are not NaN | % | Regional LSTM model, HBV model (see section 6, https://github.com/KIT-HYD/Hy2DL/tree/v1.1 , last access: 24 July 2024) |
| | validation_perc_complete | percentage of observed specific discharge values in the validation period (1965-10-01 – 1970-09-30) that are not NaN | % | |
| | testing_perc_complete | percentage of observed specific discharge values in the testing period (2001-10-01 – 2020-12-31) that are not NaN | % | |
| | NSE_lstm | Nash-Sutcliffe model efficiency coefficient of the LSTM in the testing period | – | |
| | NSE_hbv | Nash-Sutcliffe model efficiency coefficient of the HBV model in the testing period | – | |

519

520 References

521 Acuña Espinoza, E., Loritz, R., Álvarez Chaves, M., Bäuerle, N., and Ehret, U.: To bucket or not to bucket? Analyzing the
 522 performance and interpretability of hybrid hydrological models with dynamic parameterization, *Hydrology and Earth
 523 System Sciences*, 28, 2705–2719, <https://doi.org/10.5194/hess-28-2705-2024>, 2024.

524 Adam, J. C., Clark, E. A., Lettenmaier, D. P., and Wood, E. F.: Correction of global precipitation products for orographic
 525 effects, *J. Clim.*, 19, 15–38, <https://doi.org/10.1175/JCLI3604.1>, 2006.

526 Addor, N., Newman, A. J., Mizukami, N., and Clark, M. P.: The CAMELS data set: catchment attributes and meteorology
527 for large-sample studies, *Hydrology and Earth System Sciences*, 21, 5293–5313, <https://doi.org/10.5194/hess-21-5293-2017>,
528 2017.

529 Bergström, S. and Forsman, A.: Development of a Conceptual Deterministic Rainfall-runoff Model, *Hydrology Research*, 4,
530 147–170, <https://doi.org/10.2166/nh.1973.0012>, 1973.

531 Brunner, M. I., Slater, L., Tallaksen, L. M., and Clark, M.: Challenges in modeling and predicting floods and droughts: A
532 review, *WIREs Water*, 8, <https://doi.org/10.1002/wat2.1520>, 2021.

533 CLC: Corine Land Cover <https://doi.org/10.2909/960998c1-1870-4e82-8051-6485205ebbac> (last access: 24 July 2024),
534 2018.

535 Clerc-Schwarzenbach, F. M., Selleri, G., Neri, M., Toth, E., van Meerveld, I., and Seibert, J.: HESS Opinions: A few camels
536 or a whole caravan?, *EGUsphere* [preprint], <https://doi.org/10.5194/egusphere-2024-864>, 2024.

537 Coxon, G., Addor, N., Bloomfield, J. P., Freer, J., Fry, M., Hannaford, J., Howden, N. J. K., Lane, R., Lewis, M., Robinson,
538 E. L., Wagener, T., and Woods, R.: CAMELS-GB: hydrometeorological time series and landscape attributes for 671
539 catchments in Great Britain, *Earth System Science Data*, 12, 2459–2483, <https://doi.org/10.5194/essd-12-2459-2020>, 2020.

540 Dolich, A., Espinoza, E. A., Ebeling, P., Guse, B., Götte, J., Hassler, S., Hauffe, C., Kiesel, J., Heidbüchel, I., Mälicke, M.,
541 Müller-Thomy, H., Stölzle, M., Tarasova, L., & Loritz, R.: CAMELS-DE: hydrometeorological time series and attributes for
542 1582 catchments in Germany (1.0.0) [Data set]. Zenodo. <https://doi.org/10.5281/zenodo.13837553>, 2024

543 Dolich, A.: CAMELS-DE Processing Pipeline, Zenodo, <https://doi.org/10.5281/zenodo.13842287>, 2024

544 Droogers, P. and Allen, R. G.: Estimating reference evapotranspiration under inaccurate data conditions, *Irrig. Drain. Syst.*,
545 16, 33–45, <https://doi.org/10.1023/A:1015508322413>, 2002.

546 DWD-HYRAS: <https://www.dwd.de/DE/leistungen/hyras/hyras.html> (last access: 25 March 2024), 2024.

547 Ebeling, P., Kumar, R., Lutz, S. R., Nguyen, T., Sarrazin, F., Weber, M., Büttner, O., Attinger, S., and Musolff, A.:
548 QUADICA: water QUALity, DIScharge and Catchment Attributes for large-sample studies in Germany, *Earth System Science*
549 *Data*, 14, 3715–3741, <https://doi.org/10.5194/essd-14-3715-2022>, 2022.

550 Eiselt, K.-U., Kaspar, F., Mölg, T., Krähenmann, S., Posada, R., and Riede, J. O.: Evaluation of gridding procedures for air
551 temperature over Southern Africa, *Advances in Science and Research*, 14, 163–173,
552 <https://doi.org/10.5194/asr-14-163-2017>, 2017.

553 EU-DEM: Copernicus GLO-30 DEM, <https://doi.org/10.5270/esa-c5d3d65> (last access: 24 July 2024), 2022.

554 Färber, C., Plessow, H., Kratzert, F., Addor, N., Shalev, G., & Looser, U.: GRDC-Caravan: extending the original dataset
555 with data from the Global Runoff Data Centre (0.2) [Data set]. Zenodo. <https://doi.org/10.5281/zenodo.10074416>, 2023.

556 Feng, D., Liu, J., Lawson, K., & Shen, C.: Differentiable, learnable, regionalized process-based models with multiphysical
557 outputs can approach state-of-the-art hydrologic prediction accuracy. *Water Resources Research*, 58, e2022WR032404.
558 <https://doi.org/10.1029/2022WR032404>, 2022.

559 Heberger, M.: delineator.py: Fast, accurate watershed delineation using hybrid vector- and raster-based methods and data
560 from MERIT-Hydro (v1.3). Zenodo. <https://doi.org/10.5281/zenodo.10143149>, 2023.

561 HGM250: Hydrogeological Map of Germany (1:250,000), [https://gdk.gdi-de.org/geonetwork/srv/api/records/](https://gdk.gdi-de.org/geonetwork/srv/api/records/61ac4628-6b62-48c6-89b8-46270819f0d6)
562 [61ac4628-6b62-48c6-89b8-46270819f0d6](https://gdk.gdi-de.org/geonetwork/srv/api/records/61ac4628-6b62-48c6-89b8-46270819f0d6) (last access: 24 July 2024), 2019.

563 Hochreiter, S., & Schmidhuber, J.: Long short-term memory. *Neural Computation*, 9(8), 1735–1780.
564 <https://doi.org/10.1162/neco.1997.9.8.1735>, 1997.

565 Hochreiter, S.: The vanishing gradient problem during learning recurrent neural nets and problem solutions. *International*
566 *Journal of Uncertainty, Fuzziness and Knowledge-Based Systems*, 06(02), 107–116.
567 <https://doi.org/10.1142/s0218488598000094>, 1998.

568 Houska, T., Kraft, P., Chamorro-Chavez, A., and Breuer, L.: SPOTting Model Parameters Using a Ready-Made Python
569 Package, *PLOS ONE*, 10, e0145180, <https://doi.org/10.1371/journal.pone.0145180>, 2015.

570 Höge, M., Kauzlaric, M., Siber, R., Schönenberger, U., Horton, P., Schwanbeck, J., Floriancic, M. G., Viviroli, D., Wilhelm,
571 S., Sikorska-Senoner, A. E., Addor, N., Brunner, M., Pool, S., Zappa, M., and Fenicia, F.: CAMELS-CH:
572 hydro-meteorological time series and landscape attributes for 331 catchments in hydrologic Switzerland, *Earth System*
573 *Science Data*, 15, 5755–5784, <https://doi.org/10.5194/essd-15-5755-2023>, 2023.

574 HYRAS-DE-HURS: Raster data set of daily mean relative humidity in % for Germany - HYRAS-DE-HURS, Version v5.0,
575 [https://opendata.dwd.de/climate_environment/CDC/grids_germany/multi_annual/hyras_de/humidity/DESCRIPTION_GRD_](https://opendata.dwd.de/climate_environment/CDC/grids_germany/multi_annual/hyras_de/humidity/DESCRIPTION_GRD_DEU_P30Y_RH_HYRAS_DE_en.pdf)
576 [DEU_P30Y_RH_HYRAS_DE_en.pdf](https://opendata.dwd.de/climate_environment/CDC/grids_germany/multi_annual/hyras_de/humidity/DESCRIPTION_GRD_DEU_P30Y_RH_HYRAS_DE_en.pdf) (last access: 24 July 2024), 2022.

577 HYRAS-DE-PRE: Raster data set of daily sums of precipitation in mm for Germany - HYRAS-DE-PRE, Version v5.0,
578 [https://opendata.dwd.de/climate_environment/CDC/grids_germany/daily/hyras_de/precipitation/DESCRIPTION_GRD_](https://opendata.dwd.de/climate_environment/CDC/grids_germany/daily/hyras_de/precipitation/DESCRIPTION_GRD_DEU_PID_RR_HYRAS-DE_en.pdf)
579 [U_PID_RR_HYRAS-DE_en.pdf](https://opendata.dwd.de/climate_environment/CDC/grids_germany/daily/hyras_de/precipitation/DESCRIPTION_GRD_DEU_PID_RR_HYRAS-DE_en.pdf) (last access: 24 July 2024), 2022.

580 HYRAS-DE-RSDS: Raster data set of daily mean global radiation in W/m² for Germany - HYRAS-DE-RSDS,
581 https://opendata.dwd.de/climate_environment/CDC/grids_germany/daily/hyras_de/radiation_global/DESCRIPTION_GRD_DEU_PID_RAD_G_HYRAS_DE_en.pdf (last access: 24 July 2024), Version v3.0, 2023.

583 HYRAS-DE-TAS: Raster data set of daily mean temperature in °C for Germany - HYRAS-DE-TAS, Version v5.0,
584 https://opendata.dwd.de/climate_environment/CDC/grids_germany/daily/hyras_de/air_temperature_mean/DESCRIPTION_GRD_DEU_PID_T2M_HYRAS_DE_en.pdf (last access: 24 July 2024), 2022.

586 HYRAS-DE-TASMAX: Raster data set of daily maximum temperature in °C for Germany - HYRAS-DE-TASMAX,
587 Version v5.0,
588 https://opendata.dwd.de/climate_environment/CDC/grids_germany/monthly/hyras_de/air_temperature_max/DESCRIPTION_GRD_DEU_P1M_T2M_X_HYRAS_DE_en.pdf (last access: 24 July 2024), 2022.

590 HYRAS-DE-TASMIN: Raster data set of daily minimum temperature in °C for Germany - HYRAS-DE-TASMIN, Version
591 v5.0,
592 https://opendata.dwd.de/climate_environment/CDC/grids_germany/daily/hyras_de/air_temperature_min/DESCRIPTION_RD_DEU_PID_T2M_N_HYRAS_DE_en.pdf (last access: 24 July 2024), 2022.

594 Klingler, C., Schulz, K., and Herrnegger, M.: LamaH-CE: LARge-SaMple DATA for Hydrology and Environmental Sciences
595 for Central Europe, Earth System Science Data, 13, 4529–4565, <https://doi.org/10.5194/essd-13-4529-2021>, 2021.

596 Kratzert, F., Klotz, D., Shalev, G., Klambauer, G., Hochreiter, S., and Nearing, G.: Towards learning universal, regional, and
597 local hydrological behaviors via machine learning applied to large-sample datasets, Hydrology and Earth System Sciences,
598 23, 5089–5110, <https://doi.org/10.5194/hess-23-5089-2019>, 2019.

599 Lehner, B., Roth, A., Huber, M., Anand, M., Grill, G., Osterkamp, N., Tubbesing, R., Warmedinger, L., and Thieme, M.:
600 HydroSHEDS v2.0 – Refined global river network and catchment delineations from TanDEM-X elevation data, EGU
601 General Assembly 2021, online, 19–30 Apr 2021, EGU21-9277, <https://doi.org/10.5194/egusphere-egu21-9277>, 2021

602 Muñoz-Sabater, J., Dutra, E., Agustí-Panareda, A., Albergel, C., Arduini, G., Balsamo, G., Boussetta, S., Choulga, M.,
603 Harrigan, S., Hersbach, H., Martens, B., Miralles, D. G., Piles, M., Rodríguez-Fernández, N. J., Zsoter, E., Buontempo, C.,
604 and Thépaut, J.-N.: ERA5-Land: a state-of-the-art global reanalysis dataset for land applications, Earth System Science Data,
605 13, 4349–4383, <https://doi.org/10.5194/essd-13-4349-2021>, 2021.

606 Poggio, L., de Sousa, L. M., Batjes, N. H., Heuvelink, G. B. M., Kempen, B., Ribeiro, E., and Rossiter, D.: SoilGrids 2.0:
607 producing soil information for the globe with quantified spatial uncertainty, SOIL, 7, 217–240,
608 <https://doi.org/10.5194/soil-7-217-2021>, 2021.

609 Rauthe, M., Steiner, H., Riediger, U., Mazurkiewicz, A., and Gratzki, A.: A Central European precipitation climatology Part
610 I: Generation and validation of a high-resolution gridded daily data set (HYRAS), *Meteorologische Zeitschrift*, 22, 235–256,
611 <https://doi.org/10.1127/0941-2948/2013/0436>, 2013.

612 Razafimaharo, C., Krähenmann, S., Höpp, S., Rauthe, M., and Deutschländer, T.: New high-resolution gridded dataset of
613 daily mean, minimum, and maximum temperature and relative humidity for Central Europe (HYRAS), *Theoretical and
614 Applied Climatology*, 142, 1531–1553, <https://doi.org/10.1007/s00704-020-03388-w>, 2020.

615 Seibert, J., HBV Light Version 2. User’s Manual. Department of Physical Geography and Quaternary Geology, Stockholm
616 University, Stockholm, https://www.geo.uzh.ch/dam/jcr:c8afa73c-ac90-478e-a8c7-929eed7b1b62/HBV_manual_2005.pdf
617 (last access: 19. September 2024), 2005

618 Speckhann, G. A., Kreibich, H., and Merz, B.: Inventory of dams in Germany, *Earth System Science Data*, 13, 731–740,
619 <https://doi.org/10.5194/essd-13-731-2021>, 2021.

620 VG250: Verwaltungsgebiete 1:250 000 - Stand 01.01., [https://gdk.gdi-de.org/geonetwork/srv/api/records/
621 93a98c5c-cf03-4a95-bf0a-54001fbf3949](https://gdk.gdi-de.org/geonetwork/srv/api/records/93a98c5c-cf03-4a95-bf0a-54001fbf3949) (last access: 24 July 2024), 2023.

622 Vrugt, J. A.: Markov chain Monte Carlo simulation using the DREAM software package: Theory, concepts, and MATLAB
623 implementation, *Environmental Modelling & Software*, 75, 273–316, <https://doi.org/10.1016/j.envsoft.2015.08.013>,
624 2016.

625 Yamazaki, D., Ikeshima, D., Sosa, J., Bates, P. D., Allen, G. H., and Pavelsky, T. M.: MERIT Hydro: A High-Resolution
626 Global Hydrography Map Based on Latest Topography Dataset, *Water Resources Research*, 55, 5053–5073,
627 <https://doi.org/10.1029/2019wr024873>, 2019.

628 Yamazaki, D., Ikeshima, D., Tawatari, R., Yamaguchi, T., O’Loughlin, F., Neal, J. C., Sampson, C. C., Kanae, S., and Bates,
629 P. D.: A high-accuracy map of global terrain elevations, *Geophysical Research Letters*, 44, 5844–5853,
630 <https://doi.org/10.1002/2017gl072874>, 2017.